

COMPARISON OF DYNAMIC AND STATIC ENVIRONMENTALLY ASSISTED  
CRACKING TEST METHODS FOR ALUMINIUM ALLOYS

M. G. Burns\*, D. Sarchamy\*, L. Schra†, R. Braun††

ABSTRACT

Three aerospace laboratories performed environmental testing of aluminium alloy 7010 T651 under constant exposure to substitute seawater solution (ASTM D1141). One laboratory employed a dynamic (rising displacement) compact tension specimen test method with the control and monitoring of the test being provided by a 'back face strain' measurement system. The two remaining laboratories employed a constant displacement, bolt loaded double cantilever beam method. All test pieces were extracted from a single material plate, with crack planes being at the mid-thickness. The results of the static and dynamic tests are in good agreement. However, the dynamic method required shorter test duration.

INTRODUCTION

The definition of a standardised method for dynamic testing to determine the threshold stress intensity for stress corrosion cracking ( $K_{Isc}$ ) and crack growth rate (da/dt) of alloys under environmental conditions was the objective of the European Community contract MAT1 CT 930038 [1]. This involved a number of organisations from across the Community testing several material/environment systems by a variety of test methods. Of these organisations three aerospace industry laboratories, British Aerospace (BAe) Airbus, Nationaal Lucht- en Ruimtevaartlaboratorium (NLR), and Deutsches Zentrum für Luft- und Raumfahrt (DLR), undertook to test aluminium alloy 7010 - T651 in a substitute seawater solution.

NLR and DLR performed reference testing using a double cantilever beam (DCB) specimen under constant displacement loading, whilst BAe employed a 25 mm thickness compact tension (CT) specimen under rising displacement loading. The CT specimens were fitted with a strain gauge on the 'back face', with the output being monitored to provide both the test data record and the test rate control parameter. This paper describes the test procedures, and compares the results of the static DCB tests with the dynamic CT tests.

MATERIAL

The material employed in this part of the programme was from a single 90 mm thick plate of aluminium alloy 7010 - T651. The material composition and properties were characterised by the University of Hanover. The composition, by percent weight, was determined to be:

Al - 6.41 Zn - 2.43 Mg - 1.74 Cu - 0.087 Fe - 0.04 Ti - 0.036 Si - 0.01 Mn - 0.01 Cr - 0.005 Ni - 0.14 Zr.

\* *Test & Development Engineering, British Aerospace Airbus, Filton, U.K.*

† *Loads & Fatigue, Nationaal Lucht- en Ruimtevaartlaboratorium, Amsterdam, Netherlands*

†† *Institute of Materials Research, Deutsches Zentrum für Luft- und Raumfahrt, Köln, Germany*

The mechanical properties are detailed below:

Yield Stress	$\sigma_y$	436	MPa
Ultimate Stress	$\sigma_{ult}$	588	MPa
Elongation	A	4.7	%
Reduction of Area	Z	5.0	%
Young's Modulus	E	70	GPa
Hardening Coefficient	n	0.15	
Slope of Blunting Line	bl	2120	
Fracture toughness in air	$K_{Ic}$	20	MPa $\sqrt{m}$

All specimens were extracted such that the crack plane would be at the plate mid-thickness, and crack propagation would be in the longitudinal (L) direction. Loading was in the short transverse (S) direction.

#### SPECIMENS

The DCB specimen is illustrated in Figure 1a, and the CT specimen in Figure 1b. A calibrated strain gauge was fitted at the centre of the back face of each CT specimen. This face, the gauge and the connection wires were then coated with PR1422 sealant to ensure isolation from the environment.

All specimens were precracked to a nominal initial crack length of 30 and 50 mm (DCB specimens), or 26 mm (CT specimens).

The test solution was ASTM D1141 substitute seawater solution, without heavy element additions.

#### TEST PROCEDURES

**Double Cantilever Beam.** The initial displacement at the front face,  $v_0$ , was calculated from the defined initial applied stress intensity factor  $K_{II}$  as follows:

- i) The load line displacement  $v_{LL}$  was calculated from  $K_{II}$  using

$$K_{II} = \left( \frac{E \cdot H \cdot v_{LL}}{4} \right) \cdot \left[ \frac{\sqrt{\{3H(a+0.6H)^2 + H^3\}}}{(a+0.6H)^3 + H^2 \cdot a} \right] \quad \{1\}$$

where H is the specimen 'half height', and a is the crack length (see Fig. 1a).

- ii) The crack mouth displacement  $v_0$  was calculated from  $v_{LL}$  using

$$v_0 = \left( \frac{2a + 3C_1}{2a} \right) \cdot v_{LL} \quad \{2\}$$

where  $C_1$  is the distance from the crack mouth to the load line.

Specimens were bolt-loaded to the required displacement. The bolt, insert, and surrounding area were coated to prevent galvanic coupling, then immersed in the solution with the crack tip 5 mm below the surface. The solution was replaced at 14-day intervals, with evaporation loss being compensated for by additions of distilled water. The pH was monitored before and after solution replacement, initial pH being 8.2, decreasing to 8.10 - 8.15. The corrosion potential was monitored, but no consistent trend was identified.

The specimens were removed from solution at intervals (initially daily, decreasing to once every two weeks in the later stages) to monitor crack length. The total exposure period was 10 months. On completion of exposure the side face crack lengths were

measured. The clip gauge was kept in place during unloading, and the displacement monitored. The specimen was then mounted in a tensile test machine, and reloaded to the same crack mouth displacement as measured at the start of unloading. The load at this point was considered to be that at completion of testing. On breaking open the specimen, the final crack lengths and, where possible, the fatigue precrack lengths, were measured (5 point average).

The stress intensity factor at test termination was calculated in two ways :

- i) From the final crack length measured from the fracture surface,  $a_{rfs}$ , and the load line displacement by equation {1},
- ii) From  $a_{rfs}$  and the load P in the bolt at test termination, using

$$K = \frac{P \cdot a}{B \cdot H^{1.5}} (3.46 + 2.38 \frac{H}{a}) \quad \{3\}$$

Compact Tension Specimens. The accuracy and reliability of the BFS monitoring/control system was demonstrated by preparing a number of specimens with fine wire-cut pseudocracks of various lengths. These were subjected to several loading/unloading cycles, the front face displacement and BFS output being monitored. The output was calibrated according to these results, confirming formulae (see below) which were then incorporated into the control software. Recommendations for determination of displacement rate were given in the document "Guidelines for Fracture Mechanics SCC Testing" [2], and corresponding strain rates calculated from the proving trial data. The control software allowed the test to be divided into stages so that following the initial 'load and hold' period (see below), the displacement rate control was via the BFS output.

The test clevises and loading pins were coated with electrically insulating ceramic. Any remaining metallic surfaces were masked. The specimens were mounted in a test machine with a vertical loading direction (Figure 2). The chamber working capacity was 3 litres, circulation being at a rate of 1 litre/hour from a 12.5 litre reservoir (aerated). The solution was replaced every 14 days. An initial preload of 0.5 KN was applied for 24 hours to allow the development of a microclimate at the crack tip. The system then applied load so that the BFS value increased at the required rate. Onset of crack extension was determined by examination of the test record (generated during testing) which included the instantaneous BFS output, calculated crack length and K values. Following testing the fracture surface crack length was measured by 9-point average, and the  $K_{Isc}$  value calculated by standard fracture mechanics methods.

#### BACK FACE STRAIN ANALYSIS

The proving trials referred to above confirmed the relationship :

$$BFS = A \left( \frac{a}{W} \right) \cdot P$$

Normalising P, we get  $P^* = P / (B \cdot W \cdot E)$

$$\text{So,} \quad BFS = A^* \left( \frac{a}{W} \right) \cdot P^* \quad \{4\}$$

$$\text{Where} \quad A^* \left( \frac{a}{W} \right) = \{BFS/P\} \cdot \{B \cdot W \cdot E\} \quad \{5\}$$

$A^* \left( \frac{a}{W} \right)$  is independant of specimen dimensions and material for CT geometries when so normalised.

Curve fitting from experimental results enabled the following derivation,

$$\left(\frac{a}{W}\right) = 0.03661 + 0.08687(A^*) - 7.3928(10^{-3})(A^*)^2 + 4.1197(10^{-4})(A^*)^3 - 1.3521(10^{-5})(A^*)^4 + 2.3520(10^{-7})(A^*)^5 - 1.66546(10^{-9})(A^*)^6 \quad \{6\} [3]$$

$$\text{or} \quad A^* = 1379.458535 + 1.3539.4792\left(\frac{a}{W}\right) - 52316.7945\left(\frac{a}{W}\right)^2 + 99962.1591\left(\frac{a}{W}\right)^3 - 94457.6398\left(\frac{a}{W}\right)^4 + 35498.0672\left(\frac{a}{W}\right)^5 \quad \{7\} [4]$$

**BFS** = Back Face Strain, B = specimen thickness, W = specimen width,  
E = Young's Modulus, and P = load.

Equations {6} and {7} include a correction for the plastic zone size.

## RESULTS

The results obtained by the DCB static tests performed by NLR and DLR were very similar, as might be expected from use of a standard method.

NLR [5] tested four specimens from an initial stress intensity ( $K_{II}$ ) of 15 MPa√m, and four from 10 MPa√m. It was found that the threshold stress intensity for seven of these specimens fell into the range 5 - 7 MPa√m, with the eighth having a value of 4 MPa√m.

DLR [6] tested six specimens from  $K_{II}$  values of 10 to 15 MPa√m. The threshold stress intensity values derived fell into the range 4.5 to 6.5 MPa√m.

Crack growth rates at close to the threshold stress intensity, calculated from optical observation, were in the range  $4 \times 10^{-10}$  to  $9 \times 10^{-10}$  m/s.

The results obtained from the dynamic CT tests demonstrated the importance of identifying the correct strain rate. The first test, performed at a rate of 0.06 microstrain per minute ( $\mu\epsilon/\text{min}$ ) - which equates to approximately 1.8 micron per hour - resulted in sudden failure at a stress intensity of 11.9 MPa√m. The test data printout, however, indicated that very slow crack extension had begun at a stress intensity of 11.6 MPa√m. The minute differences in the displacement/load rates would not have been easily detected without reference to the BFS data.

Reducing the strain rate allowed the optimum rate of 0.008  $\mu\epsilon/\text{min}$  to be identified, based on performing tests at rates of 0.006 to 0.06  $\mu\epsilon/\text{min}$ .

At the test rate of 0.008  $\mu\epsilon/\text{min}$ , the threshold stress value was 5.4 MPa√m, with the values at 0.006 and 0.010  $\mu\epsilon/\text{min}$  being 7.9 and 8.4 MPa√m respectively. The trend is illustrated in Figure 3.

Crack growth rates near threshold, calculated from the BFS-derived crack length and elapsed time between readings (included on the data print-out), were of the order of  $10^{-9}$  m/s.

These results were compared with those for crack lengths measured from the side face, and from the fracture surface crack length measurements (where possible, since the exact point of transition from fatigue to stress corrosion was very difficult to identify for this material). The values were, in each case, 10 - 15 % higher than those derived from the BFS system.

CONCLUSIONS

The results of the static and dynamic tests show good agreement provided that the optimum loading rate is used in the dynamic tests. For this alloy/environment system, the optimum dynamic test rate is of the order of 0.008 microstrain per minute (0.24 micron per hour load line displacement). The back face strain method of monitoring and control has proved to be both sensitive and accurate. If this series of tests had relied on visual identification of the crack length at the onset of environmental cracking, positive results would have been difficult to determine, owing to the indistinct transition between fatigue and stress corrosion zones.

The added advantage of being able to load the specimen vertically (since this is the orientation in which test machines in the majority of laboratories will be), and not having to rely on clip gauge readings - instead having calculation of the crack length, crack growth rate, and stress intensity value built into the monitoring/control software - simplifies testing.

Further modification of the control software would allow the onset of crack growth to be identified, and a constant K state to be applied automatically to allow accurate crack growth rates to be derived.

The reduction in time for completion of a test was significant. Whereas the 'static' DCB test had a duration of 10 months, the dynamic CTS test, at optimum rate, took 40 days to the onset of crack extension, and could be terminated at any point thereafter, depending on the crack growth rate information required. This time could be reduced further by applying a faster initial loading rate to a level of approximately half that corresponding to the threshold stress intensity value.

On the other hand, in most cases testing at different loading rates is necessary to define the optimum rate for establishing  $K_{I,sec}$ . Also, in the DCB static test method, more specimens may be tested at the same time without the need for equipment capable of realising low loading rates.

REFERENCES

- [1] EC Contract MAT1 CT 930038, "Characterization of Susceptibility of Metallic Materials to Environmentally Assisted Cracking". 1995.
- [2] Dietzel, W., "Guidelines for Fracture Mechanics SCC Testing.", under EC Contract MAT1 CT 930038, 1995.
- [3] M'Whinnie, R., "Comparison of Crack Length Measurement Techniques.", Submission for BSc (Hons), Paisley University, 1990.
- [4] Sarchamy, D., "Stress Corrosion Cracking of Pre-cracked BS1501 - 161 Steel in Contaminated Liquid Ammonia Under Constant and Slow Monotonic Loading.", Submission for PhD, Paisley University, 1988.
- [5] Schra, L., "The Influence of Testing Parameters on Stress Corrosion Crack Growth in the High Strength Aluminium Alloy 7010 - T651.", NLR Report TP 96710 U, 1997.
- [6] Braun, R., "Fracture Mechanics SCC Testing of the Alloy AA 7010 in the Tempers T651 and T7451 using DCB Specimens.", DLR Report, 1997.

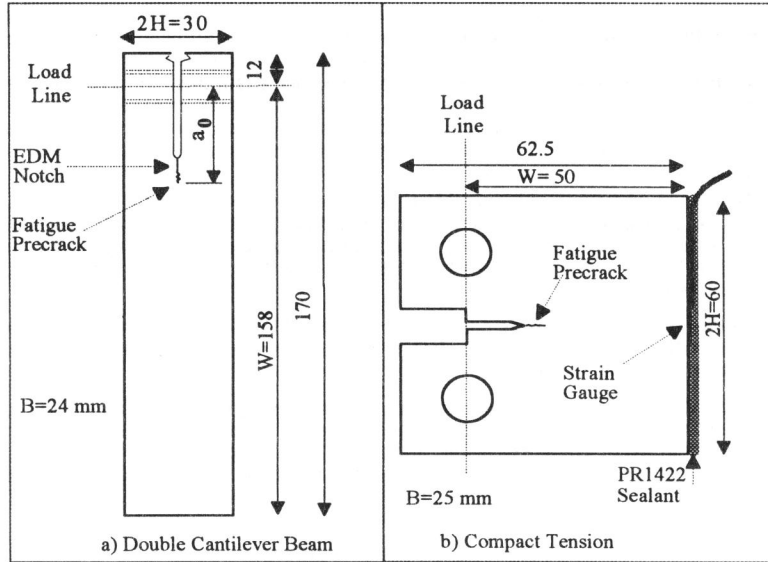


Figure 1 - Test Specimen Geometry

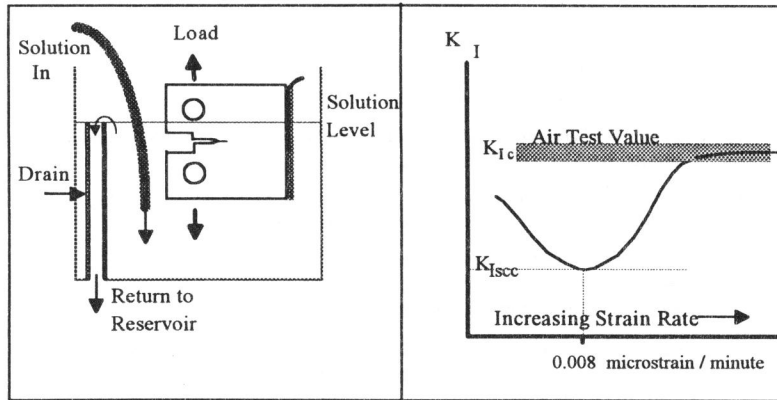


Figure 2 - Loading Orientation Within The Chamber

Figure 3 - Trend of Threshold Stress Intensity Value with Strain Rate